

Observation of the XY^- Abstraction Products in the Ion–Molecule Reactions $X^- + RY \rightarrow XY^- + R$: An Alternative to the S_N2 Mechanism at Suprathermal Collision Energies

Donna M. Cyr,[†] M. Georgina Scarton,[†] Kenneth B. Wiberg,[†] Mark A. Johnson,^{*,†} Shinji Nonose,[‡] Jun Hirokawa,[‡] Hideki Tanaka,[‡] Tamotsu Kondow,[‡] Robert A. Morris,[§] and A. A. Viggiano[§]

Contribution from the Sterling Chemistry Laboratory, Department of Chemistry, Yale University, New Haven, Connecticut 06511, Department of Chemistry, School of Science, The University of Tokyo, Hongo, Bunkyo-ku, Tokyo 113, Japan, and Phillips Laboratory/GPID, Geophysics Directorate, 29 Randolph Road, Hanscom Air Force Base, Massachusetts 01731-3010

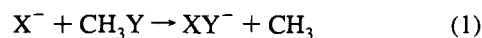
Received May 4, 1994[⊗]

Abstract: We report the formation of dihalide products from the endothermic gas-phase ion–molecule reaction of Cl^- with CH_3Br at suprathermal collision energies using both guided ion beam and selected ion flow drift tube (SIFDT) techniques. The cross sections for the $Cl^- + CH_3Br$ reactions were determined using the guided ion beam apparatus over a center-of-mass collision energy range of 2–15 eV with the $ClBr^-$ product displaying a maximum near 7 eV. This result is found to be in good agreement (when convoluted with the appropriate velocity distribution) with the rate constant measured by the SIFDT. ICl^- and I_2^- are also found for the $Cl^- + CH_3I$ and $I^- + RI$ reactions at elevated collision energies (≤ 1.5 eV) in the SIFDT. The rates for halide displacement are found to be insensitive to collision energy. These results indicate that attack on the C–X bond may *not* provide an efficient alternative to the S_N2 mechanism for halide exchange in the asymmetric $X^- + CH_3Y$ systems. This conclusion is supported by *ab initio* calculations (MP2LANL10Z level) which indicate that $ClBr^-$ can be formed by collinear attack at the halogen through a $Cl \cdots Br \cdots CH_3$ intermediate.

I. Introduction

The gas-phase ion–molecule reactions between halide anions and methyl halides have been extensively studied over the past 20 years,^{1–28} and the S_N2 reactive encounters at thermal energies are well-known to occur *via* Walden inversion. In this process,

the Walden inversion barrier is lowered by the electrostatic attraction between collision partners, forming the well-known ion–dipole double minima in the surface. Interestingly, the entropically constrained S_N2 pathway is the only mechanism for halide exchange reported for thermal gas-phase collisions, with only indirect evidence for front-side attack on the C–X bond inferred from the isotope exchange rate in the $Cl^- + CH_3Cl$ system at high (≥ 1 eV) collision energy.⁴ One of the signatures of front-side attack should be the formation of XY^- dihalide “stripping” or abstraction products:



which are typically between 1 and 2 eV endothermic,²⁹ explaining why it has not been reported in room temperature afterglow experiments. Recently, photoexcitation of the stable $I^- \cdots CH_3Br$ and $I^- \cdots CH_2Br_2$ ion–dipole exit channel complexes (as

[†] Yale University.

[‡] The University of Tokyo.

[§] Hanscom Air Force Base.

[⊗] Abstract published in *Advance ACS Abstracts*, January 15, 1995.

(1) Bader, R. F. W.; Duke, A. J.; Messer, R. R. *J. Am. Chem. Soc.* **1973**, *95*, 7715.

(2) Olmstead, W. N.; Brauman, J. I. *J. Am. Chem. Soc.* **1977**, *99*, 4219.

(3) Wilbur, J. L.; Brauman, J. I. *J. Am. Chem. Soc.* **1991**, *113*, 9699.

(4) Barlow, S. E.; Van Doren, J. M.; Bierbaum, V. M. *J. Am. Chem. Soc.* **1988**, *110*, 7240.

(5) DePuy, C. H.; Gronert, S.; Mullin, A.; Bierbaum, V. M. *J. Am. Chem. Soc.* **1990**, *112*, 865.

(6) Bohme, D. K.; Raksit, A. B. *Can. J. Chem.* **1985**, *63*, 3007.

(7) Graul, S. T.; Bowers, M. T. *J. Am. Chem. Soc.* **1991**, *113*, 9696.

(8) Shi, Z.; Boyd, R. J. *J. Am. Chem. Soc.* **1990**, *112*, 6789.

(9) Carrion, F.; Dewar, M. J. S. *J. Am. Chem. Soc.* **1984**, *106*, 3531.

(10) Dougherty, R. C.; Dalton, J.; Roberts, J. D. *Org. Mass Spectrosc.* **1974**, *8*, 77.

(11) Gronert, S. *J. Am. Chem. Soc.* **1993**, *115*, 652.

(12) Vande Linde, S. R.; Hase, W. L. *J. Phys. Chem.* **1990**, *94*, 6148.

(13) Gertner, B. J.; Whitnell, R. M.; Wilson, K. R.; Hynes, J. T. *J. Am. Chem. Soc.* **1991**, *113*, 74.

(14) Cyr, D. M.; Posey, L. A.; Bishea, G. A.; Han, C.-C.; Johnson, M. A. *J. Am. Chem. Soc.* **1991**, *113*, 9697.

(15) Cyr, D. M.; Bishea, G. A.; Scarton, M. G.; Johnson, M. A. *J. Chem. Phys.* **1992**, *97*, 5991.

(16) Cyr, D. M.; Bishea, G. A.; Han, C.-C.; Posey, L. A.; Johnson, M. A. *Soc. Photo-Opt. Instrum. Eng. (SPIE) Proc.* **1992**, *1638*, 74.

(17) Chandrasekhar, J.; Smith, S. F.; Jorgensen, W. L. *J. Am. Chem. Soc.* **1985**, *107*, 154.

(18) Caldwell, G.; Magnera, T. F.; Kebarle, P. *J. Am. Chem. Soc.* **1984**, *106*, 959.

(19) Ohta, K.; Morokuma, K. *J. Phys. Chem.* **1985**, *89*, 5845.

(20) Basilevsky, M. V.; Ryaboy, V. M. *Chem. Phys. Lett.* **1986**, *129*, 71.

(21) Riveros, J. M.; Jose, S. M.; Takashima, K. *Adv. Phys. Org. Chem.* **1985**, *21*, 197.

(22) Shaik, S. S.; Pross, A. *J. Am. Chem. Soc.* **1982**, *104*, 2708.

(23) Shaik, S. S.; Schlegel, A. B.; Wolfe, S. *Theoretical Aspects of Physical Organic Chemistry: The S_N2 Mechanism*; Wiley-Interscience: New York, 1992.

(24) Tucker, S. C.; Truhlar, D. G. *J. Am. Chem. Soc.* **1990**, *112*, 3338.

(25) Viggiano, A. A.; Paschkewitz, J. S.; Morris, R. A.; Paulson, J. F.; Gonzales-Lafont, A.; Truhlar, D. G. *J. Am. Chem. Soc.* **1991**, *113*, 9404.

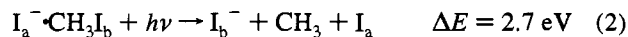
(26) Viggiano, A. A.; Morris, R. A.; Paschkewitz, J. S.; Paulson, J. F. *J. Am. Chem. Soc.* **1992**, *114*, 10477.

(27) Vetter, R.; Züllicke, L. *J. Am. Chem. Soc.* **1990**, *112*, 5136.

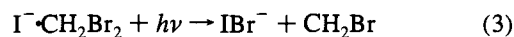
(28) VanOrden, S. L.; Pope, R. M.; Buckner, S. W. *Org. Mass Spectrosc.* **1991**, *26*, 1003.

(29) Lias, S. G.; Bartness, J. E.; Liebman, J. F.; Holmes, J. L.; Levin, R. D.; Mallard, W. G. *J. Phys. Chem. Ref. Data* **1988**, *17*(Suppl. 1), 1.

well as the complex from the identity reaction, $I^- \cdot CH_3I$ has revealed an electronically excited reaction surface located about 3.5 eV above the energy of the complexes.^{15,16} Similar to the S_N2 ground state reactions, photoexcitation of the monohalogenated (i.e. CH_3Br and CH_3I) ion-dipole complexes generates the atomic halide ions:

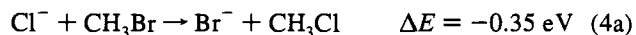


There is a difference in mechanism between photoactivation and the S_N2 reactions, however, since CH_3I does not appear to reform upon photoactivation.³⁰ Moreover, a new reaction channel producing dihalide diatomic anions, not previously observed in the ground state reactions, appears in the photoexcitation experiments which is especially pronounced for complexes involving two or more halogen atoms on the (nominally) neutral partner such as



ICR studies of the $Cl^- + CH_3Br$ reaction with up to several electron volts collision energy did not reveal the formation of $ClBr^-$ product.² We therefore initiated the present studies to establish the reactivity pattern of X^- with RY at greater than thermal collision energies using the guided ion beam apparatus at the University of Tokyo (TGIBA) to locate the energy range for the XY^- formation and then the result was cross-checked using the Selected Ion Flow Drift Tube (SIFDT) at Phillips Laboratory.

The reaction of $Cl^- + CH_3Br$ was studied over a range of center-of-mass collision energies (E_{CM}) from 2 to 15 eV in the TGIBA and from 0.8 to 1.5 eV in the SIFDT. The energetics of the reactions



indicate that these collision energy regimes should cover the range between the thermodynamic threshold for $ClBr^-$ production and the energy accessed in the photoexcitation experiments (3–4 eV). The formation of the dihalide anion from the ground state reactants appears to be general, and the rates for dihalide production from the $Cl^- + CH_3I$ and $I^- + RI$ reactions (determined in the SIFDT) are also reported here.

II. Experimental Section

The Tokyo Guided Ion Beam Apparatus (TGIBA). Reaction cross sections were first measured using the University of Tokyo guided ion beam apparatus described in detail in earlier papers.³¹ The reactant Cl^- anion is generated by electron impact ionization of a free jet containing $CHCl_3$ seeded in argon and mass selected in a quadrupole mass filter before interacting with CH_3Br in an octopole ion guide surrounded by a 12 cm long gas collision cell. This apparatus introduced a ± 1.0 eV spread in the center-of-mass collision energy, E_{CM} , after injection into the quadrupole mass filter and octopole ion guide. Product ions were collected into a magnetic sector for final mass analysis. Mass discrimination of the conversion dynode detector was taken into account in the calculation of the reaction cross sections. The typical parent beam intensities in the collision cell are on the order of $10^6 \text{ cm}^{-2} \text{ s}^{-1}$ with a beam diameter of about 0.6 cm. The pressure

in the collision cell ($\sim 10^{-4}$ Torr) resulted in less than 1% attenuation of the parent beam. Reaction cross sections for the production of $ClBr^-$ and Br^- were obtained from the slope of the product intensity plotted versus CH_3Br pressure at each collision energy with a relative uncertainty of about 10%.

The Phillips Laboratory Selected Ion Flow Drift Tube (SIFDT). The rate constants for the reactions of Cl^- with CH_3Br and CH_3I , and I^- with RI ($R = \text{methyl, ethyl, } n\text{-propyl, isopropyl}$) were measured with the SIFDT apparatus at Phillips Laboratory at the Hanscom Air Force Base in Massachusetts. The experimental details have been described previously,^{32,33} and only details pertinent to the present experiment are discussed here. The primary halide ions, Cl^- (again generated by electron impact of $CHCl_3$), are extracted from the source and mass-selected by a quadrupole mass filter before injection into the flow tube with helium buffer gas. The reactants (CH_3Br and RI) were introduced through downstream inlets and their reactivities measured over a 50 cm drift distance as a function of reactant flow rate or concentration.

Accurate mass calibration was needed to ensure that the dihalide products were XY^- and not XHY^- . This was accomplished by injecting a calibrant ion with a mass close to that of the dihalide product of interest. Note that the absence of the latter products is not surprising since their production is typically ~ 2 eV more endothermic than the halide abstraction reaction (XY^-).²⁹

In most cases, the decay of the primary ion signal with increasing reactant concentration was limited by the small rate constants combined with the high energies needed for these experiments which resulted in short reaction times. The small decays in the primary ion signal did not, in general, allow us to measure rate constants from the decline in the primary ion signal as a function of added reactant gas as is normal in SIFDT experiments. Instead, rate constants were measured by the rise in the product ion signal. Subsequently the primary ion decay could be estimated by the difference between the primary ion intensity before reaction and the integrated product ion intensities. This allowed measurement of smaller than usual rate constants but with less accuracy than is typical for SIFDT determinations. In measuring rate constants this way, one must know the mass discrimination between the primary and the secondary ions since both the initial primary ion and the product ion signals enter into the calculations. Rate constants were measured under low mass resolution where the mass discrimination in our system is less than 30%. This translates into an added uncertainty in the rate constants, which we conservatively estimate to be accurate to about a factor of 2. At lower energy, where the S_N2 channel competes with the dihalide reaction, the primary decay was large enough to measure. In this case, rate constants for the individual channels were determined by multiplying the observed overall rate constant by the branching fraction to each product channel. Mass discrimination also adds uncertainty into these data.

Ions were accelerated by applying a uniform electric field to the drift tube. The ion velocity was measured by pulsing two of the drift rings and measuring the reactant ion arrival times. From the measured drift velocity the average collision energy was determined by the Wannier expression.³⁴ Measurements were carried out for three different collision energies in the range 0.8–1.5 eV.

For most purposes, the Wannier expression has been shown to be an excellent approximation for $\langle KE_{cm} \rangle$ in drift tube experiments, and the distribution of energies can be considered Maxwellian.³⁵ However, these assumptions are probably not as accurate for the present situation. The reactions of interest occur only at high energy, a situation where the Wannier expression is less accurate and small changes in the high energy tail of the distribution can strongly affect the measured rate constants. Estimating the effect of the distribution of energies on the rate constants is beyond the scope of the present study. While this

(32) Viggiano, A. A.; Morris, R. A.; Dale, F.; Paulson, J. F.; Giles, J. F.; Smith, D.; Su, T. *J. Chem. Phys.* **1990**, *93*, 1149.

(33) Viggiano, A. A.; Morris, R. A.; Van Doren, J. M.; Paulson, J. F. *J. Chem. Phys.* **1992**, *96*, 275.

(34) Wannier, G. H. *Bell Syst. Tech. J.* **1953**, *32*, 170.

(35) Viehland, L. A.; Viggiano, A. A.; Mason, E. A. *J. Chem. Phys.* **1991**, *95*, 7286. and references therein.

(30) Cyr, D. M.; Bailey, C. G.; Serxner, D.; Johnson, M. A. The dissociative charge transfer excited state of the $I^- \cdot CH_3I$ S_N2 reaction intermediate: Photoinduced intra-cluster dissociative attachment. In *J. Chem. Phys.* **1994**, *101*, 10507.

(31) Ichihashi, M.; Hirokawa, J.; Nonose, S.; Nagata, T.; Kondow, T. *Chem. Phys. Lett.* **1993**, *204*, 219.

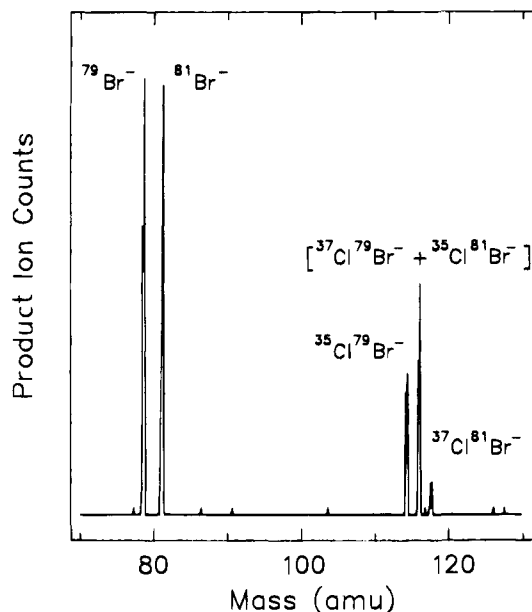


Figure 1. Product mass spectrum from the $\text{Cl}^- + \text{CH}_3\text{Br}$ reaction at ~ 2 eV center-of-mass collision energy (E_{CM}) with a collision cell pressure of 2.0×10^{-4} Torr of CH_3Br .

will prevent detailed interpretation of the data, general features such as the observation of the dihalide product and determination of the approximate rates are not affected.

III. Results

Figure 1 presents a typical TGIBA mass spectrum of the products from reaction 4 at a nominal collision energy of $E_{\text{CM}} = 2$ eV. The ClBr^- product is clearly important in this energy range, amounting to roughly 30% of the products. When the target pressure exceeds 3×10^{-4} Torr, the $\text{ClBr}^-/\text{Br}^-$ branching ratio was found to decrease with increasing reaction cell pressures, consistent with collisional dissociation of the ClBr^- product at higher pressures. The intensities of ClBr^- were found to be proportional to the pressure of the target gas, CH_3Br , at pressures lower than 3×10^{-4} Torr.

Figure 2 presents the partial cross sections for both the ClBr^- abstraction and the Br^- displacement products as a function of center-of-mass collision energy (E_{CM}). While the Br^- substitution product cross section is quite insensitive to the collision energy, the ClBr^- cross section displays a maximum near $E_{\text{CM}} = 7 \pm 1$ eV with an onset (≈ 2 eV) just above the endoergicity of this reaction channel (≈ 1.8 eV) as marked by the arrow.

Since the lower limit of the TGIBA energy range was about 1 eV, the SIFDT apparatus was used to extend the results to lower energy. For $\langle E_{\text{CM}} \rangle \leq 0.5$ eV, only the monohalide (nominally $\text{S}_{\text{N}}2$) products were observed (e.g. reaction 4a) with rate constants consistent with those found in previous reports.^{4,5,18,25} The dihalide product was observed at higher average collision energy (0.8–1.5 eV) and comprised at most 3% of the observed displacement products at the highest collision energies accessible by the SIFDT. The fact that XY^- represents a rather minor channel in this (thermal) energy range explains how this reaction escaped observation in early surveys of this energy regime.² The dihalide branching ratio determined by TGIBA at higher collision energies ($\langle E_{\text{CM}} \rangle \geq 2$ eV) indicates that the dihalide reaction channel rate constant continues to increase (see Figure 2) beyond the range of collision energies accessible by the SIFDT method.

The halide abstraction reaction rate constants (in the SIFDT experiment) were derived from the slopes of the decrease in

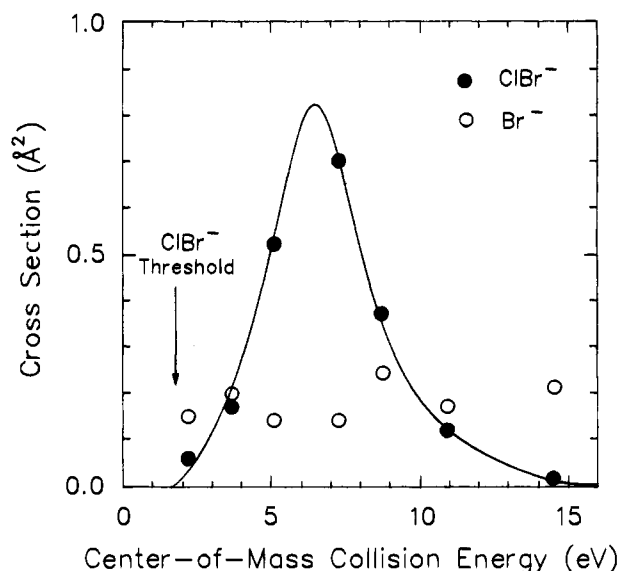


Figure 2. The absolute cross sections for the formation of the displacement product, Br^- (open circles), and the halide abstraction product, ClBr^- (solid circles), for the reaction $\text{Cl}^- + \text{CH}_3\text{Br}$, plotted as a function of center-of-mass collision energy (E_{CM}).

Table 1. Rate Constants for the Displacement and Abstraction Reactions ($\times 10^{-11} \text{ cm}^3 \text{ s}^{-1}$) as a Function of Collision Energy (eV)

collision energy ($\langle E_{\text{CM}} \rangle$)	SIFDT ^a reaction rate constant		TGIBA ^b abstraction reaction rate
	displacement	abstraction	
$\text{Cl}^- + \text{CH}_3\text{Br}$			
0.81	4.0	0.09	0.03
1.00	3.7	0.12	0.07
1.23	4.1	0.15	0.15
$\text{Cl}^- + \text{CH}_3\text{I}$			
0.91	5.5	0.11	<i>c</i>
1.39	6.1	0.19	<i>c</i>
1.57	6.4	0.24	<i>c</i>

^a Error in reported rate constants is $\pm 50\%$. ^b Calculated from TGIBA cross section data. ^c Values not calculated since cross section data are not available.

the parent ion counts (parent ion – product ion counts) plotted versus neutral reactant concentration or flow. The rate constants for both the substitution and abstraction reactions are reported in Table 1 for several collision energies.

It is possible to establish whether these two observations of XY^- kinetics are self consistent by simulating the SIFDT rate constant, $k(T_{\text{eff}})$, by averaging the cross section obtained in the TGIBA, $\sigma(E_{\text{CM}})$, over a Maxwell–Boltzmann distribution of relative collision energies:

$$k(T_{\text{eff}}) \propto \int v \sigma(E_{\text{CM}}) \cdot P(E_{\text{CM}}) dE_{\text{CM}} \quad (5a)$$

$$k(T_{\text{eff}}) = \left(\frac{1}{\pi\mu}\right)^{1/2} \cdot \left(\frac{2}{k_{\text{B}}T}\right) \int_0^{\infty} \sigma(E_{\text{CM}}) E_{\text{CM}} e^{-E_{\text{CM}}/k_{\text{B}}T} dE_{\text{CM}} \quad (5b)$$

as outlined by Ervin *et al.*³⁶ The effective temperature, T_{eff} , is estimated from the average collision energy $\langle E_{\text{CM}} \rangle$ using the Wannier formula:³⁴

$$\frac{3}{2} k_{\text{B}} T_{\text{eff}} = \frac{1}{2} v_{\text{d}}^2 \frac{(m_i + m_b) m_n}{(m_i + m_n)} + \frac{3}{2} k_{\text{B}} T \quad (6)$$

where m_i = mass of reactant ion, m_b = mass of SIFDT buffer

Table 2. Abstraction Reaction Rate Constants for $I^- + RI \rightarrow I_2^- + R$

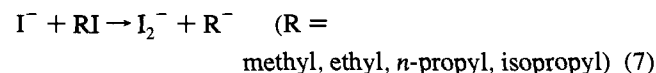
reaction	rate constant $\times 10^{-13}$ ($\text{cm}^3 \text{s}^{-1}$) ($E_{\text{CM}} = 1.0 \text{ eV}$)
$I^- + \text{CH}_3\text{I}$	3.5
$I^- + \text{CH}_3\text{CH}_2\text{I}$	8.5
$I^- + \text{CH}_3\text{CH}_2\text{CH}_2\text{I}$	7.5
$I^- + \text{CH}_3\text{CHICH}_3$	8.0

gas (He), m_n = mass of reactant neutral, v_d = drift velocity, and k_B = Boltzmann constant. A spline fit of the reaction cross section (shown as a solid line drawn through the data in Figure 2) is used as the functional form for the cross section in the calculation of eq 5b.

The rate constant for ClBr^- formation calculated from the TGIBA cross sections is in surprisingly good agreement with the SIFDT data at 1.23 eV (see Table 1). This agreement in the energy range where the two experiments overlap indicates that the non-Maxwellian nature of the energy distributions does not severely affect the rate constants in the drift tube. At lower energies the agreement is less good (9×10^{-13} vs 3×10^{-13} $\text{cm}^3 \text{s}^{-1}$ for SIFDT relative to TGIBA at $E_{\text{CM}} = 0.81 \text{ eV}$), perhaps due to the uncertainty in extrapolating the TGIBA data outside its energy range, although the difference is not alarming considering that the SIFDT rate constants are only good to a factor of 2. In the reactions of both $\text{Cl}^- + \text{CH}_3\text{Br}$ and $\text{Cl}^- + \text{CH}_3\text{I}$ a trend of increasing abstraction with increasing kinetic energy is observed (note that the trends are more reliable than the absolute rate constants).

A similar calculation was not performed for the $\text{S}_{\text{N}}2$ reaction since the cross section at low energies (<2 eV), where the displacement products dominate, was not measured in the TGIBA apparatus. It is possible, nonetheless, to recover the observed substitution cross section in the TGIBA at high collision energy by extrapolating the low-energy cross section (using the observed SIFDT reaction efficiency), σ^0 , with a simple $E^{-1/2}$ dependence, where $\sigma(E) \sim \sigma^0 E^{-1/2}$.³⁷ The cross section thus calculated for reaction 4a (0.27 \AA^2) is actually in good agreement with the observed TGIBA cross section ($\sigma_{\text{obs}}(2\text{eV}) = 0.18 \pm 0.02 \text{ \AA}^2$) at a collision energy of 2.0 eV.

We also investigated the influence of substituents around the α -carbon in the RI series by SIFDT:

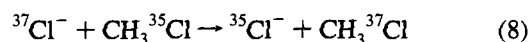


While the rate constant appears to be distinguishably smaller for dihalide production from methyl iodide (3.5×10^{-13} $\text{cm}^3 \text{s}^{-1}$) than for the longer chain species (8.0×10^{-13} $\text{cm}^3 \text{s}^{-1}$), it is basically insensitive to the nature of the R group (see Table 2) in the experimental uncertainty (about a factor of 2).

IV. Discussion

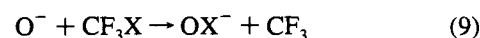
One obtains the following picture of the reaction of halides with halomethanes as a function of collision energy. At low energy, reactive collisions must find the narrow pathway over the $\text{S}_{\text{N}}2$ transition state through backside attack, while attack at the C-X bond occurs at high collision energies producing the abstraction channel. The halide abstraction reaction implies an exit channel complex $(X-Y)^-\text{CH}_3$ which could, in principle, lead to an alternative pathway for halide exchange. In fact, such a complex has already been invoked to explain the rapid

increase in the isotope exchange rate coefficients for the process⁴



at around 0.5 eV average translational energy in a SIFT-drift apparatus similar to the one employed here (from the point of view of the velocity distributions of the reactants). The authors interpreted this onset using the formalism for translationally driven reactions developed by Chesnavich and Bowers³⁸ to infer an activation energy of about 2 eV. This energy is consistent with the formation of a Cl_2^-CH_3 complex which opens a second pathway for halide exchange in addition to the $\text{S}_{\text{N}}2$ mechanism. Unfortunately, the Cl_2^- product implied by this model was not observed up to 2 eV, but Cl_2^- formation is more endothermic (2.3 eV) than ClBr^- formation (1.8 eV) observed here. The absence of the Cl_2^- abstraction product from the $\text{Cl}^- + \text{CH}_3\text{Cl}$ reaction was also noted in our SIFDT experiments at $E_{\text{CM}} \leq 1.5 \text{ eV}$. Thus, the isotope scrambling experiment appears to anticipate the formation of the new products before the channel becomes energetically accessible, as discussed in Ferguson's endothermic trapping model.³⁹ In spite of the mechanistic similarity between the Cl_2^-CH_3 and ClBr^-CH_3 intermediates, it is significant to note that the abrupt rise in the displacement rate observed in the $\text{Cl}^- + \text{CH}_3\text{Cl}$ reaction is *not* observed in the reactions of Cl^- with CH_3Br and CH_3I considered here (see Table 1 and Figure 2). It is noteworthy that the observed rate constants for the $\text{Cl}^- + \text{CH}_3\text{Br}$ reaction reported here are about an order of magnitude larger than that *extrapolated* from the data in ref 25 which covered the range $0.02 < E < 0.1 \text{ eV}$, so there could be an increase outside the range of the current measurements.

The endothermic abstraction products reported here have been observed in the related series of reactions⁴⁰



where the channel is exothermic. In fact, reaction 9 dominates the $\text{S}_{\text{N}}2$ product even though the latter is more exothermic by about a factor of 10. This, combined with the large rate constant for reaction 9, indicates the OX^- channel proceeds without a barrier.

An interesting aspect of the cross sections presented in Figure 2 is the rather narrow peak in the ClBr^- cross section. The onset just above 2 eV is easily understood as a line-of-centers type increase above the endoergic threshold, but the reason for the peak at $\approx 7 \text{ eV}$ is not obvious. No other species were observed to rise commensurate with the decrease above 7 eV as would be expected for a product breakdown curve. One possibility, of course, is that the nascent ClBr^- is breaking apart into $\text{Cl}^- + \text{Br}$ at high energy so the experiment is blind to the "new" channel. In any case, the nature of the 7 eV peak would appear to be a fruitful avenue for future work on this problem.

To evaluate the plausibility of formation of XY^- by direct attack at the halogen, we carried out a series of *ab initio* calculations to investigate the energetics of collinear attack of Cl^- on the bromine end of CH_3Br . These calculations were carried out using the LANL1DZ basis set that is of double- ζ quality and used effective core potentials for chlorine and bromine. Preliminary calculations at the MP2/LANL1DZ level found a weakly bound complex ($\Delta E = -2.5 \text{ kcal/mol}$, not corrected for the basis set superposition error, but including zero-point energies) with $R(\text{Cl}-\text{Br}) = 3.15 \text{ \AA}$ and $R(\text{Br}-\text{C}) = 2.062 \text{ \AA}$ [note that, $R(\text{Br}-\text{C}) = 2.028 \text{ \AA}$ in the isolated reactant]. The

(37) Su, T.; Bowers, M. T. Classical Ion-Molecule Collision Theory. In *Gas Phase Ion Chemistry*; Bowers, M. T., Ed.; Academic Press: New York, 1979; Vol. 1, p 87.

(38) Chesnavich, W. J.; Bowers, M. T. *J. Phys. Chem.* **1979**, *83*, 900.

(39) Ferguson, E. E. *J. Chem. Phys.* **1984**, *81*, 742.

(40) Morris, R. A. *J. Chem. Phys.* **1992**, *97*, 2372.

approach of the chlorine was found to be collinear with the Br–C bond, indicating that the reaction can proceed by attack on the bromine. Such processes are known to occur in constrained reactions and have recently been inferred in the reaction of 1,3-diiodobicyclo[1.1.1]pentane with OH⁻.⁴¹ Collinear attack is intuitive since it is unlikely that this reaction proceeds *via* a pentavalent carbon species (recall that the analogous trihalide anions are linear⁴²), and the transition state is probably Cl^{δ-}··Br^{δ-}··CH₃ in nature. At shorter Cl–Br distances, the activated complex began to assume diradical character, and calculations were carried out at the UMP2/LANL1DZ level. The energy was found to increase, reaching the energy of the separated products as a limit. Thus, it appears that the reverse reaction has little if any activation energy, consistent with the observation based on reaction 9. A calculation of the vibrational modes when the C–Br distance was 3.6 Å found only one imaginary mode indicating retention of the complex's C_{3v} symmetry along this reaction coordinate. The overall process was further examined at QCISD/LANL1DZ,

(41) Wiberg, K. B.; McMurdie, N. *J. Am. Chem. Soc.* **1991**, *113* 8995.

(42) Downs, A. J.; Adams, C. J. Chlorine, Bromine, Iodine and Astatine. In *Comprehensive Inorganic Chemistry*; Bailar, J. C., Jr., Emeleus, H. J., Nyholm, R., Trotman-Dickerson, A. F., Eds.; Pergamon Press, Oxford, 1973; Vol. 2, p 1112.

but no significant change in the calculated relative energies was found. These results indicate that a direct mechanism is plausible at these high collision energies.

Summarizing, the reactive pathways inferred from these measurements indicate that abstraction may *not* provide an efficient alternative to the Walden inversion mechanism for halide exchange between different halides at elevated collision energy and may occur *via* attack at the halogen in a collinear arrangement rather than front-side attack on carbon.

Acknowledgment. M.A.J. thanks the National Science Foundation under grants CHE-9207894 and INT-9016913, as well as discussions about unpublished results with Profs. S. Graul, M. T. Bowers, and J. I. Brauman. Dr V. Bierbaum's helpful comments on this work were also appreciated. Acknowledgment is made to the donors of the Petroleum Research Fund, administered by the ACS for partial support of this research. T.K. thanks JSPS MPCR-212 grants for international collaboration and the Grant-in-Aid for Scientific Research in Priority Areas by the ministry of Education, Science and Culture. The PL authors acknowledge helpful discussions with Dr. John Paulson.

JA941388Z